

is also possible and would have less electrostatic repulsion in the formation of the transition state, but the proton would also make it more difficult for Cl^- to leave. We propose that the factor of 3.3×10^4 difference in reactivity between OCl^- and HOCl is due to a change of mechanism from O atom transfer to Cl^+ transfer.

The previous ^{18}O -labeling experiments² with sulfite and hypochlorite were actually carried out in 0.2 M HCl where HOCl , Cl_2 , SO_3H^- , and SO_2 were all present and the reaction mechanisms would very likely be completely different than is the case in NaOH solutions or in $\text{HCO}_3^-/\text{CO}_3^{2-}$ buffer.

Conclusions

The rate of oxidation of SO_3^{2-} with HOCl is more than 4 orders

of magnitude faster than the rate with OCl^- . A shift in mechanism from O atom transfer for OCl^- to Cl^+ transfer for HOCl is proposed to account for the huge increase in reactivity. Below pH 11 the rate of the oxidation can be limited by proton-transfer reactions. A reactive intermediate species, HOClSO_3^{2-} , is proposed, which reacts to form ClSO_3^- . The HOCl reactivity with $\text{SO}_3^{2-} > \text{I}^- > \text{Br}^-$ is highly dependent on the nucleophilicity of these anions.

Acknowledgment. This work was supported by National Science Foundation Grants CHE-8616666 and CHE-8720318.

Registry No. SO_3^{2-} , 14265-45-3; HOCl , 7790-92-3; OCl^- , 14380-61-1.

Contribution from the Department of Chemistry,
The Florida State University, Tallahassee, Florida 32306-3006

Kinetics of Dissociation of Trivalent Actinide Chelates of TMDTA

Anthony C. Muscatello, Gregory R. Choppin,* and Willem D'Olieslager†

Received December 15, 1987

Measurements by a radiotracer technique show that the dissociation of TMDTA (trimethylenediamine-*N,N*-tetraacetic acid) chelates with Am, Cm, Bk, Cf, and Eu proceeds through an acid-catalyzed pathway. The rates of dissociation of $\text{An}(\text{TMDTA})^-$ are 2 orders of magnitude faster than those of the corresponding EDTA chelates, presumably due to the greater lability of the nitrogen atom in the six-membered nitrogen-metal-nitrogen ring of TMDTA chelates. The rate of dissociation also decreased with decreasing metal ion radius. A proton-catalyzed mechanism similar to that for dissociation of EDTA complexes of lanthanide and actinide cations is consistent with the rate data.

Introduction

Studies of the kinetics of chelate complexation of the f elements are complicated by the ionic nature of the bonding in these complexes, as this results in relatively short-lived processes. The polydentate nature of the amino carboxylate complexes slows the rates of dissociation, allowing easier investigation. In these chelates, in which both carboxylate and amine donors are involved, questions arise about the rate-controlling processes in the bond formation and dissociation. Optical and NMR spectroscopies as well as metal exchange have been used to study the kinetics of lanthanide chelation.¹ The radioactive nature of the analogous trivalent actinide elements has restricted their study. However, the actinide systems that have been investigated show close similarity to the lanthanide complexes with the same ligands.

The exchange of trivalent actinides, An^{3+} , with $\text{La}(\text{EDTA})^-$ complexes follows reversible first-order kinetics.²⁻⁵ The rate equation for the exchange contained two terms, one dependent and one independent of the hydrogen ion concentration. The hydrogen ion dependent term was associated with proton-catalyzed dissociation of the lanthanide chelate. The free ligand then reacted with the actinide ion. The acid-independent term was interpreted as being due to a mechanism in which the actinide ion directly attacks and displaces the lanthanide in the complex.

Other studies of transplutonium element chelates include an investigation by El-Rawi⁶ of the exchange kinetics of Am(III), Cm(III), and Cf(III) with lanthanum chelates that also reported acid-dependent and acid-independent terms in the rate equation. Makarova et al.⁷ investigated Am(DCTA) and Cm(DCTA) dissociation rates using an electromigration method,⁸ while Sullivan et al.⁹ measured Am(DCTA) formation rates by stopped-flow spectrophotometry and dissociation rates by Cu(II) exchange. Both of these studies found acid-dependent and acid-independent pathways in the dissociative mechanism.

To better understand the factors involved in chelation kinetics, we have studied the dissociation of Eu(III), Am(III), Cm(III), Bk(III), and Cf(III) chelates of TMDTA (trimethylenedi-

aminetetraacetic acid). TMDTA (also known as PDTA or 1,3-propanediaminetetraacetic acid) complexes would have one more carbon atom in the nitrogen-metal-nitrogen chelate ring than would EDTA complexes. Comparison of the stability constants of $\text{Ln}(\text{EDTA})^-$ and $\text{Ln}(\text{TMDTA})^-$ indicated that TMDTA complexes probably would have dissociation half-lives of a 1 min or less. Consequently, a solvent extraction system that allowed fast sampling was used. The development of this technique has been described previously.¹⁰ We have also previously determined the stability constants of the chelates of Am, Cm, Bk, and Cf with TMDTA.¹¹

Experimental Section

Reagents. Trioctylphosphine oxide, TOPO, from Eastman, was used without further purification. A 0.5 M solution was prepared by dissolving a weighed sample of TOPO in warm *n*-dodecane and diluting to volume. The solution was pre-equilibrated with an acetate buffer at a pH similar to that of the reaction solution (nonbuffered 0.5 M solutions of TOPO are supersaturated at room temperature).

TMDTA, trimethylenediaminetetraacetic acid, was synthesized by the method of Tanaka and Ogino¹² as revised by Ogino et al.¹³ The pre-

- (1) Breen, P. J.; Horrocks, W. DeW., Jr.; Johnson, K. A. *Inorg. Chem.* **1986**, *25*, 1968.
- (2) D'Olieslager, W.; Choppin, G. R. *J. Inorg. Nucl. Chem.* **1971**, *33*, 127.
- (3) D'Olieslager, W.; Choppin, G. R.; Williams, K. R. *J. Inorg. Nucl. Chem.* **1970**, *32*, 3605.
- (4) Choppin, G. R.; Williams, K. R. *J. Inorg. Nucl. Chem.* **1973**, *35*, 4255.
- (5) Williams, K. R.; Choppin, G. R. *J. Inorg. Nucl. Chem.* **1974**, *36*, 1849.
- (6) El-Rawi, H. Report KFK-1927; Karlsruhe Nuclear Research Center: Karlsruhe, FRG, 1974.
- (7) Makarova, T. P.; Stepanov, A. V.; Gedeonov, A. D.; Maksimova, A. M. *Radiokhimiya* **1976**, *18*, 794; *Sov. Radiochem. (Engl. Transl.)* **1976**, *18*, 677.
- (8) Stepanov, A. V. *Zh. Fiz. Khim.* **1973**, *47*, 1769; *Russ. J. Phys. Chem. (Engl. Transl.)* **1973**, *47*, 993.
- (9) Sullivan, J. C.; Nash, K. L.; Choppin, G. R. *Inorg. Chem.*, **1978**, *17*, 3374.
- (10) Choppin, G. R.; Muscatello, A. C.; D'Olieslager, W. In *The Rare Earths in Modern Science and Technology*; McCarthy, G. J., Rhyne, J. J., Eds.; Plenum Press: New York, 1978; p 135.
- (11) Choppin, G. R.; Muscatello, A. C. *Inorg. Chim. Acta* **1985**, *109*, 67.
- (12) Tanaka, N.; Ogino, H. *Bull. Chem. Soc. Jpn.* **1964**, *37*, 877.
- (13) Ogino, H.; Takahashi, M.; Tanaka, N. *Bull. Chem. Soc. Jpn.* **1970**, *43*, 424.

* Present address: Department of Chemistry, The Catholic University of Leuven, Leuven, Belgium.

cipitate was recrystallized from 24% ethanol and titrated with standardized NaOH, which confirmed it to be 100% TMDTA. A weighed amount of the acid was dissolved in 2 equiv of 0.1 M NaOH to make a 0.01 M stock solution of TMDTA. Sodium acetate buffer stock (0.200 M) was prepared by adding a sufficient amount of 1.0 M NaOH to 1.00 M acetic acid (Anachemia Chemicals, Acculute) to achieve the desired pH when the system was diluted to the correct volume. Reagent grade sodium chloride (Matheson Coleman and Bell) was dried at 110 °C and dissolved to make a 1.00 M stock solution. Distilled water, deionized with mixed-bed ion-exchange-resin cartridges (Barnstead Ultrapure), was used for all solutions.

Celite 545 (Sargent-Welch Scientific Co. and Fisher Scientific Co.) was made hydrophobic¹⁰ by contacting with dimethyldichlorosilane in acetone solution and evaporating. The TOPO solution was sorbed onto the Celite to make a supported solvent extractant.

Radiotracers. The tracers ²⁴¹Am, ²⁴⁴Cm, ²⁴⁹Bk, ²⁵²Cf, and ^{152,154}Eu were obtained from Oak Ridge National Laboratory and purified by cation-exchange techniques. The purified tracers were evaporated to dryness and redissolved in 0.01 M HCl to a specific activity of about 25 000 cpm/μL. ²⁴¹Am, ²⁴⁴Cm, and ²⁵²Cf were checked for radiochemical purity by α spectrometry. ^{152,154}Eu was checked by γ spectrometry.

Kinetics. An aqueous reaction mixture was prepared by mixing aliquots of TMDTA and acetate buffer solution with sufficient NaCl solution to obtain an ionic strength of 0.1 M. The pH was adjusted with dilute NaOH or HCl. The procedure used in the experiments has been described in detail in the earlier paper. The reaction solution is mixed by magnetic stirring with the TOPO-coated Celite 545 and a small aliquot of the radiotracer added to start the reaction. Small aliquots of the slurry are removed with rapid filtration. During a run, less than 10% (total) of the mixture is removed for sampling. ^{152,154}Eu was counted in a NaI(Tl) scintillation (well) counter. ²⁴¹Am, ²⁴⁴Cm, ²⁴⁹Bk, and ²⁵²Cf were counted with a Packard 3320 liquid scintillation counter.

The pH of the solutions was measured by using a combination electrode and a Beckman Research pH meter. NaCl was used instead of NaClO₄ as the supporting electrolyte in the reaction solutions to avoid drift in the pH reading due to the precipitation of KClO₄ in the salt bridge. In addition, use of NaCl allowed direct comparison of these results with those of previous kinetic studies^{3,4} of Eu(EDTA)⁻ and An(EDTA)⁻.

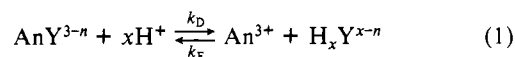
Since concentrations of the other species in solution were used in calculations, the concentration of hydrogen ion, pcH, was determined from the activity measurements (i.e., pH). The combination electrodes were calibrated with hydrochloric acid solutions of known concentration (0.1–0.0001 M) and constant ionic strength. The straight line found for a plot of pcH vs. pH was fitted by a linear-regression program to obtain the relationship pcH = pH – 0.109 (μ = 0.1 M). The estimated error in pcH was ±3%.

Before each series of pH measurements, the electrode was standardized with a 0.05 M potassium hydrogen phthalate buffer (pH = 4.008).

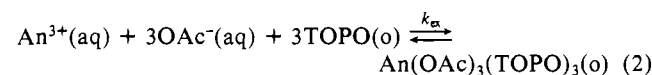
The kinetic data were processed by computer, and the slope, the intercept, the 95% confidence limits of the slope, and the standard error of the intercept were determined by a linear-regression routine. Normally, single experiments were done for each radioisotope at each TMDTA and each hydrogen ion concentration. The pH range studied was 5.5–6.3.

Results

The An(TMDTA)⁻ chelate forms upon addition of the An³⁺ tracer to the reaction mixture, and the subsequent extraction by TOPO measures the dissociation of this complex. The equation for the dissociation of an amino carboxylate chelate, Yⁿ⁻, with an actinide, An³⁺, can be written as



where k_D is the dissociation rate constant and k_F is the formation rate constant. Removal of the free actinide from the aqueous phase by fast extraction with the TOPO sorbed on the Celite would drive the reaction almost to completion. The equations for the TOPO extraction have been given previously.¹⁰ However, the hydrogen ion dependence included in those equations was shown subsequently not to be present. The extraction reaction is



where (aq) denotes a species in the aqueous phase and (o) denotes a species in the organic phase. Assuming a first-order proton-

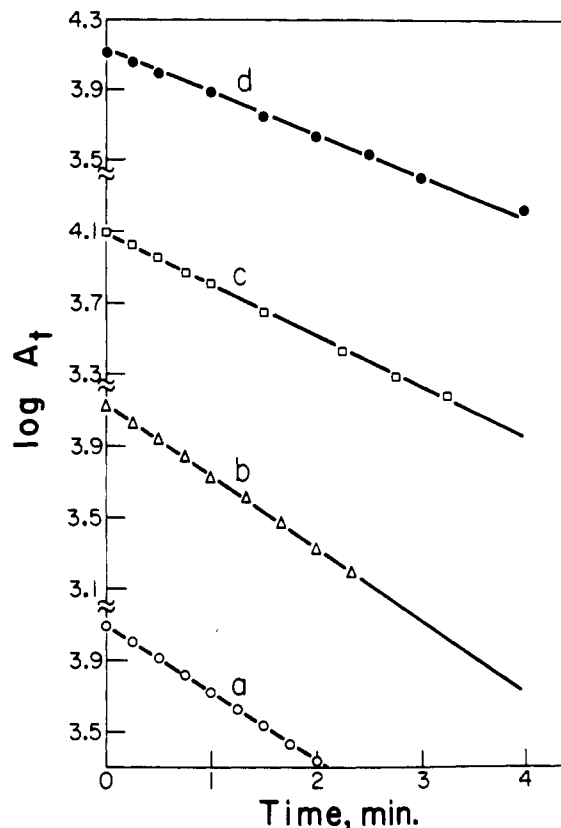


Figure 1. Plots of $\log A_t$ vs time for the extraction of ^{152,154}Eu from TMDTA solutions ([OAc]_T = 0.02 M, I = 0.1 M (NaCl), 25 °C). [TMDTA]_T (M), [H⁺] (M): (a) 2×10^{-4} , 6.55×10^{-7} ; (b) 4×10^{-4} , 8.43×10^{-7} ; (c) 8×10^{-4} , 7.23×10^{-7} ; (d) 2×10^{-3} , 8.07×10^{-7} .

catalyzed dissociation of the complex, we obtain as the overall rate expression

$$-d[\text{AnY}]/dt = k_{\text{obs}}[\text{AnY}] = \frac{k_D[\text{H}^+][\text{AnY}]k_{\text{ex}}[\text{OAc}][\text{TOPO}]}{k_F[\text{Y}]_T + k_{\text{ex}}[\text{OAc}][\text{TOPO}]} \quad (3)$$

where $[\text{Y}]_T$ = total concentration of Y. This relation is valid because the formation rate of the chelate is of the same magnitude as that of the extraction rate. The dissociation rate constant, k_D , is obtained from

$$[\text{H}^+]/k_{\text{obs}} = 1/k_D + \frac{k_F[\text{Y}]_T}{k_D k_{\text{ex}}[\text{OAc}][\text{TOPO}]} \quad (4)$$

A plot of $[\text{H}^+]/k_{\text{obs}}$ vs $[\text{Y}]_T$ yields a straight line with an intercept of $1/k_D$.

To confirm the validity of this solvent extraction technique for measuring kinetics, we studied the dissociation of Am(EDTA)⁻. Applying eq 4 to the data gave a value of $149 \pm 8 \text{ M}^{-1} \text{ s}^{-1}$ for k_D . This value is in excellent agreement with the value found from a study of Am³⁺/Eu(EDTA)⁻ exchange using a cation-exchange separation technique ($139 \pm 13 \text{ M}^{-1} \text{ s}^{-1}$).⁴ This observation eliminates the probability of extraction of the chelate, which apparently occurs for La(EDTA)⁻ from solutions of much lower pH.¹⁴

At the upper end of the pH range of the experiments, the extraction of Eu³⁺ from the TMDTA solutions had a linear dependence of $\ln A_t$ (A_t = radioactivity of Eu³⁺ in aqueous phase at time t) on time (Figure 1), which is interpreted as being due to pseudo-first-order dissociation of the Eu(TMDTA)⁻ complex. However, in more acidic solutions and for the actinide-TMDTA systems, the $\ln A_t$ vs t data were not linear. These curves could, however, be resolved into two straight-line components, as shown in Figure 2. In all of these solutions, the metal ion is >99.5%

(14) Al-Dabbagh, F. H.; Bullock, J. I. *J. Less-Common Met.* **1986**, *125*, 75.

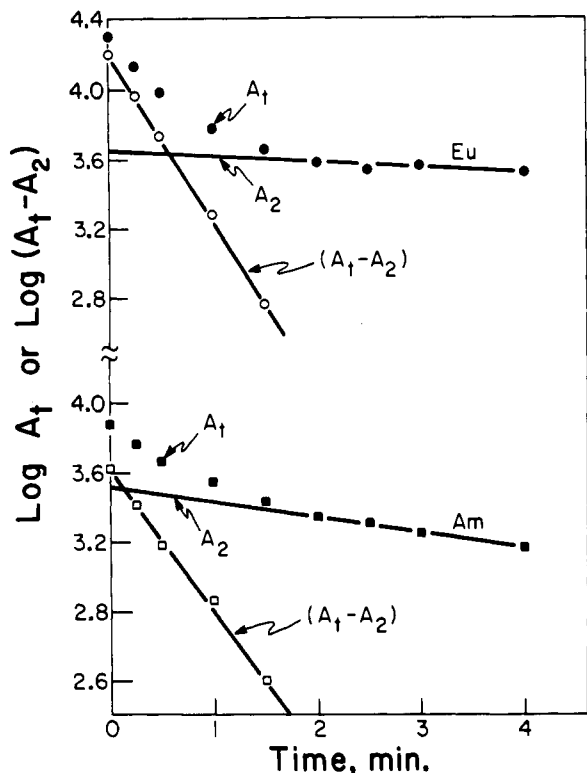


Figure 2. Plots of $\log A_1$ and $\log (A_1 - A_2)$ vs time for the extraction of $^{152,154}\text{Eu}$ and ^{241}Am from TMDTA solutions ($[\text{OAc}]_{\text{T}} = 0.02 \text{ M}$, $I = 0.1 \text{ M}$ (NaCl), 25°C). Eu: $[\text{TMDTA}]_{\text{T}} = 2 \times 10^{-3} \text{ M}$, $[\text{H}^+] = 2.20 \times 10^{-6} \text{ M}$. Am: $[\text{TMDTA}]_{\text{T}} = 2 \times 10^{-3} \text{ M}$, $[\text{H}^+] = 8.18 \times 10^{-7} \text{ M}$.

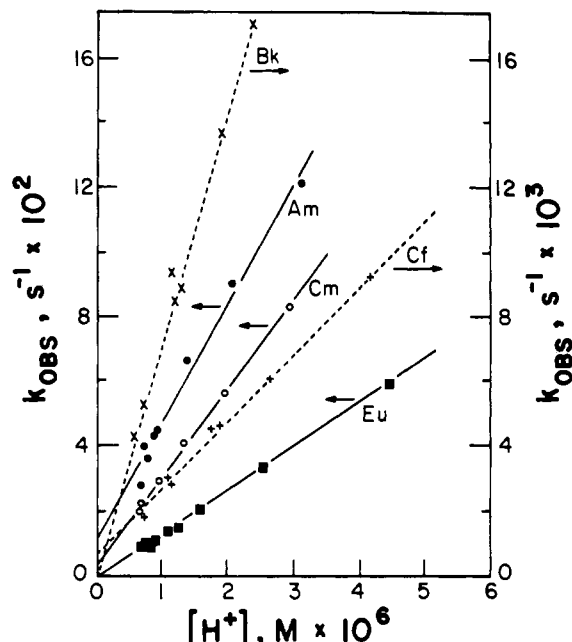


Figure 3. Plots of k_{obs} vs $[\text{H}^+]$ for $\text{An}(\text{TMDTA})^-$ dissociation kinetics ($[\text{OAc}]_{\text{T}} = 0.02 \text{ M}$, $I = 0.1 \text{ M}$ (NaCl), 25°C). Eu: $[\text{TMDTA}]_{\text{T}} = 1 \times 10^{-3} \text{ M}$. Am through Cf: $[\text{TMDTA}]_{\text{T}} = 2 \times 10^{-4} \text{ M}$.

in the TMDTA chelate form. The initial component of the resolved $\text{Eu}(\text{TMDTA})^-$ curve in Figure 2 was consistent with the rate expected for first-power dependence on hydrogen ion concentration extrapolated from the linear curves of Figure 1. These curves were all shown to be dependent on pH.

Extractions performed in the absence of TMDTA gave data consistent with the more long-lived component. For example, extractions of Am from TMDTA solutions had long-lived kinetic components, with rates ranging from 3.8×10^{-4} to $2.9 \times 10^{-3} \text{ s}^{-1}$. By comparison, extractions of Am in the absence of TMDTA had

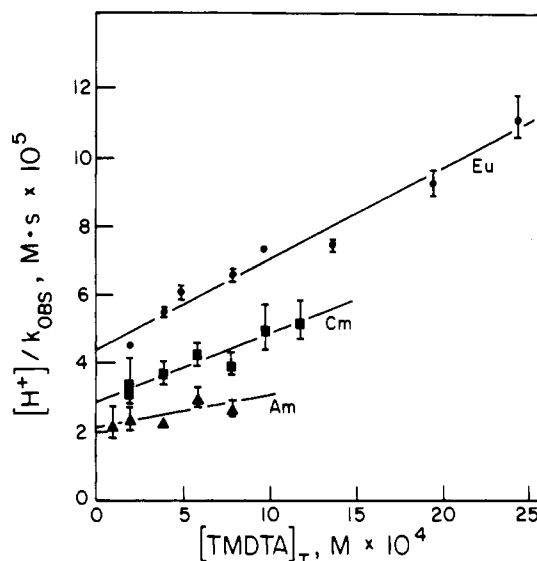


Figure 4. Plots of $[\text{H}^+]/k_{\text{obs}}$ vs $[\text{TMDTA}]_{\text{T}}$ for $\text{An}(\text{TMDTA})^-$ dissociation kinetics for Eu, Am, and Cm ($[\text{OAc}]_{\text{T}} = 0.02 \text{ M}$, $I = 0.1 \text{ M}$, 25°C). Error bars are 95% confidence limits.

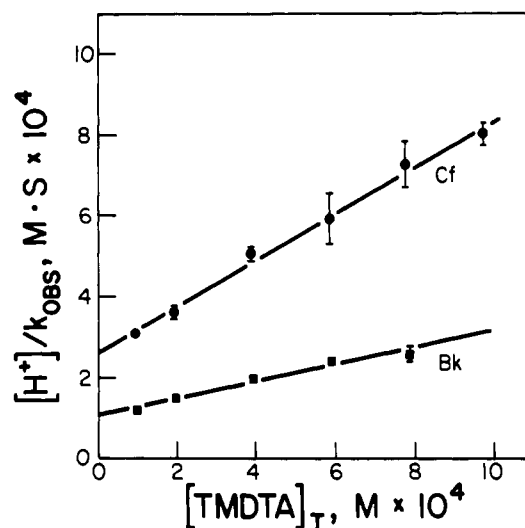


Figure 5. Plots of $[\text{H}^+]/k_{\text{obs}}$ vs $[\text{TMDTA}]_{\text{T}}$ for $\text{An}(\text{TMDTA})^-$ dissociation kinetics for Bk and Cf ($[\text{OAc}]_{\text{T}} = 0.02 \text{ M}$, $I = 0.1 \text{ M}$, 25°C). Error bars are 95% confidence limits.

long-lived components with rates that ranged from 2.8×10^{-4} to $1.7 \times 10^{-3} \text{ s}^{-1}$. In neither case was there any observable dependence on pH. Similar results were found for Eu, Cm, Bk, and Cf. A possible explanation for the long-lived component is that the extractant on the surface of the Celite rapidly equilibrates with free metal ions in solution. However, the diffusion of the TOPO-metal complex into the core of the particle may be relatively slow. At this point, the dissociation of the TMDTA is no longer rate-determining. This effect was not observed with $\text{Am}(\text{EDTA})^-$ dissociation kinetics because this rate is 100 times slower and the chelate dissociation remains rate-determining. Because the fast initial extraction onto the Celite remains constant from experiment to experiment, the data treatment method is valid for $\text{An}(\text{TMDTA})^-$ dissociation kinetics. Consequently, the initial short-lived component was analyzed for the hydrogen ion dependency of the metal-TMDTA dissociation rate.

Figure 3 shows that straight lines were obtained by plotting k_{obs} vs $[\text{H}^+]$, which indicates a first-power dependence on hydrogen ion concentration. Nonzero intercepts were obtained for Am, Cm, Bk, and Cf, due to a minor contribution from an acid-independent pathway. However, the data were insufficient to allow meaningful analysis of the kinetics of this dissociation path. Figures 4 and 5 show that $\text{An}(\text{TMDTA})^-/\text{TOPO}$ kinetics also follow eq 4. Table I summarizes the results of these plots. The inverse values of the

Table I. Intercepts, Slopes, and Extrapolated Rate Constants of $[H^+]/k_F$ Plots for $An(TMDTA)^-$ Dissociation ($I = 0.1$ M (NaCl), $T = 25$ °C, $[OAc^-] = 0.02$ M)

metal	pH(av)	intercept $\times 10^5$, s	slope $\times 10^2$, s	$10^{-4}k_D$, $M^{-1} s^{-1}$
Eu	6.120	4.37 (± 0.25)	2.63 (± 0.19)	2.29 (± 0.13)
Am	5.862	2.09 (± 0.21)	0.971 (± 0.441)	4.78 (± 0.49)
Cm	6.205	2.84 (± 0.18)	1.97 (± 0.25)	3.52 (± 0.22)
Bk	5.858	10.6 (± 1.0)	20.6 (± 2.2)	0.945 (± 0.095)
Cf	5.865	25.7 (± 1.4)	56.8 (± 2.2)	0.390 (± 0.021)

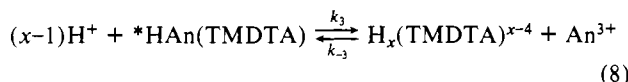
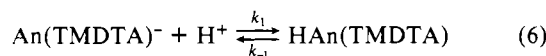
intercepts in Figures 4 and 5 correspond to the k_D values, listed in Table I.

Discussion

The pseudo-first-order kinetics observed during the extraction reaction are a consequence of the tracer-level concentrations of the actinides resulting in a constant concentration of the ligand in the course of a reaction. Also, the concentration of TMDTA, although considerably greater than that of the An^{3+} metal, is insufficient to form any $An(TMDTA)_2^{5-}$ species. Figures 4 and 5 show that the dissociation data can be expressed by the equation

$$[H^+]/k_{obs} = a + b[H_2(TMDTA)^{2-}] \quad (5)$$

Figure 3 confirms the first-power dependence on hydrogen ion concentration shown in eq 5. The protonation of the chelate is not the rate-determining step in the acid-catalyzed dissociation of the amino polycarboxylate chelate. Rather, it is the dissociation of the protonated complex that is the slow process. It has been proposed⁴ that the rate-determining step for $An(EDTA)^-$ dissociation is either (1) the dissociation of the second carboxylate group or, more likely, (2) the transfer of a proton from the carboxylate group to the nearest nitrogen atom. The TMDTA kinetics are consistent with both of these mechanisms, so the individual reactions in the overall dissociative mechanism can be written generally as:



Equations 6–8 represent respectively fast protonation of the chelate, slow conversion to an activated species, and the fast dissociation of the activated species with concomitant, immediate protonation of the ligand to form the species present at a particular pH. The extraction of the free metal ion into the organic phase is represented by eq 2. Acetate is assumed to be the coextracted anion since there would be much more actinide acetate in the solution than actinide chloride complexes and the acetate complexes can be expected to be more organophilic. Trivalent actinides and lanthanides are extracted as the TOPO trisolvates. We designate k_4 as the forward (extraction) rate constant and k_{-4} as the reverse (back-extraction) rate constant of eq 2.

Therefore, the rate of formation of $An(OAc)_3(TOPO)_3(o)$ from $An(TMDTA)^-$, $R(o)$, is the rate of formation of $HAn(TMDTA)$ multiplied by the probability of forming $*HAn(TMDTA)$ from $HAn(TMDTA)$ and by the probability of forming $An(OAc)_3(TOPO)(o)$ from An^{3+} :

$$R(o) = k_1[H^+][An(TMDTA)^-] \left(\frac{k_2}{k_2 + k_{-1}} \right) \times \left(\frac{k_3[H^+]^{x-1}}{k_3[H^+]^{x-1} + k_{-2}} \right) \times \left(\frac{k_4[OAc^-]^x[TOPO]^y}{k_4[OAc^-]^x[TOPO]^y + k_{-3}[H_x(TMDTA)^{x-4}] } \right) \quad (9)$$

$$k_{obs}[An(TMDTA)^-] = \frac{k_2K_1k_4'[H^+][An(TMDTA)^-]}{k_4' + k_{-3}[H_x(TMDTA)^{x-4}]} \quad (10)$$

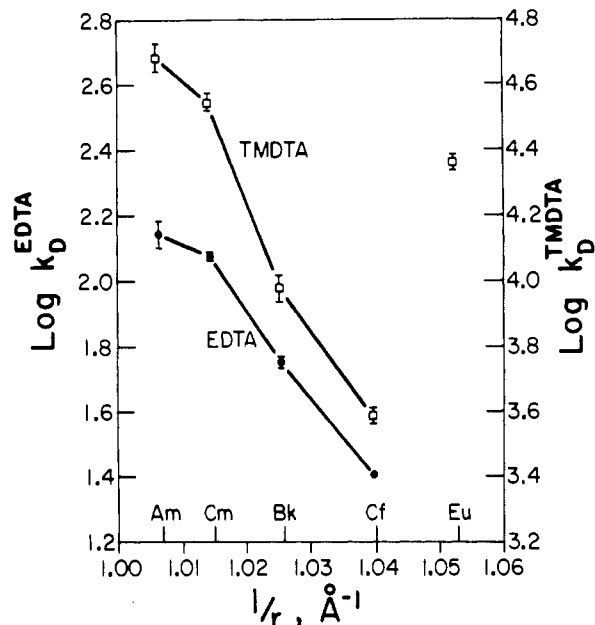


Figure 6. Plots of the rate constants of the acid-dependent dissociation pathway of AnY^- vs the reciprocal of the cationic radius.

where $K_1 = k_1/k_{-1}$ and $k_4' = k_4[OAc^-]^x[TOPO]^y$ (because $k_{-1} \gg k_2$ and $k_3[H^+]^{x-1} \gg k_{-2}$). The rate law of the reverse reaction is not considered, since >95% of the metal ion was extracted in all experiments.

As 99% of TMDTA is in the diprotonated form in the pH range of interest, eq 10 can be rearranged to give

$$\frac{k_{obs}}{[H^+]} = \frac{k_2K_1k_4'}{k_4' + k_{-3}[H_2(TMDTA)^{2-}]} \quad (11)$$

Inverting eq 11 leads to

$$\frac{[H^+]}{k_{obs}} = \frac{1}{k_2K_1} + \frac{k_{-3}[H_2(TMDTA)^{2-}]}{k_2K_1k_4'} \quad (12)$$

Equation 12 is equivalent to eq 5 if $a = 1/k_2K_1$ and $b = k_{-3}/k_2K_1k_4'$. In this case, k_D in Table I is equivalent to k_2K_1 .

The bonding in these actinide-amino carboxylate complexes is strongly electrostatic and can be expected to be proportional to the charge density of the metal cation for a given ligand. The essential linearity of plots of $\log k_D$ vs the reciprocal of the cation radii for TMDTA and EDTA in Figure 6 reflects this ionic character since $1/r$ is directly related to the cation charge density. Thus, the plots in Figure 6 show that the dissociation rate of the actinide-amino carboxylate complexes is inversely related to the strength of the ionic bonding.

In addition, it is possible to calculate the overall formation rate constants of $An(TMDTA)^-$, assuming that the reaction



is the dominant pathway. Although $H_2(TMDTA)^{2-}$ is the predominant form in this pH range, the concentration of $H(TMDTA)^{3-}$ can be calculated from the acid dissociation constants at any particular pH. From the dissociation rate constants (Table II), the corresponding stability constants, β_{101} ,¹¹ and the equation

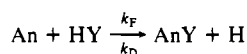
$$\beta_{101} = k_F^{HY}/k_DK_{4a} \quad (14)$$

where K_{4a} is the acid dissociation constant of $H(TMDTA)^{3-}$ (i.e., $10^{-10.39}$),¹⁵ we obtain the values listed in Table II. Analogous values for the EDTA and DCTA kinetics also are included in Table II.

In contrast to linear variation of the $\log k_D$ values, the logarithms of the formation rate constants vary in a nonlinear manner as a function of the reciprocal of the crystal radii of the cations.

(15) Martell, A. E.; Smith, R. M. *Critical Stability Constants*; Plenum Press: New York, 1974; Vol. 1.

(16) Nyssen, G. A.; Margerum, D. W. *Inorg. Chem.* **1970**, *9*, 1814.

Table II. Rate Constants ($M^{-1} s^{-1}$) for the Reaction

metal	TMDTA		DCTA (8, 14)		EDTA (4,5)	
	$10^{-7}k_F$	$10^{-4}k_D$	$10^{-8}k_F$	k_D	$10^{-10}k_F$	$10^{-2}k_D$
Am	5.5 (± 0.9)	4.78 (± 0.49)	1.2	4.4	0.59	1.39
Cm	8.8 (± 1.2)	3.52 (± 0.22)	2.4	2.8	1.0	1.10
Bk	8.8 (± 1.6)	0.95 (± 0.10)			1.2	0.57
Cf	1.3 (± 1.0)	0.39 (± 0.02)			0.85	0.25
Eu	3.2 (± 0.4)	2.29 (± 0.13)	0.34	3.2	0.32	2.28

It has been proposed that this nonlinear behavior for $\log k_F$ reflects that the hydrated radii of the actinide cations do not have a direct inverse relation with the crystal radii.¹⁷

From these data, we can see how the structure of the ligand affects the formation rate constant of amino polycarboxylate chelates. The EDTA complexes have the fastest formation rate; the slower rate for the formation of DCTA chelates may be attributed to the stereochemical rigidity imposed by the cyclohexyl ring, and that for the TMDTA chelates may be attributed to the formation of the less stable six-membered N-M-N ring (in agreement with the observations of Kustin and co-workers).^{18,19}

- (17) Jones, A. D.; Choppin, G. R. *Actinides Rev.* **1969**, *1*, 311.
 (18) Kustin, K.; Pasternak, R. F.; Weinstock, E. M. *J. Am. Chem. Soc.* **1966**, *88*, 4610.
 (19) Kowalak, A.; Kustin, K.; Pasternak, R. R.; Petrucci, S. *J. Am. Chem. Soc.* **1967**, *89*, 3216.

The relative dissociation rates also reflect the effect of the difference in stability between the five-membered N-M-N chelate ring in the EDTA complexes and the six-membered ring in the TMDTA chelates. Similarly, the stereochemical rigidity of the DCTA chelates can be invoked to explain the much lower rate of dissociation of these complexes compared to that of the An(EDTA) complexes.

Summary

A solvent extraction method has been used to study the dissociation kinetics of trivalent actinide chelates whose rate is moderately fast ($t_{1/2} < 1$ min). The dissociation of $An(TMDTA)^-$ proceeds through a proton-catalyzed pathway in which the first step is postulated to be the protonation of a carboxylate group in a fast equilibrium. The slow step is assigned to the dissociation of the nitrogen atom from the metal ion coupled to the formation of a hydrogen bond with the protonated carboxylate. The subsequent dissociation of the metal ion and the protonated ligand is rapid.

The dissociation rate constants decrease with metal ionic radius, which we attribute to decreasing nitrogen-metal bond lability. The increased chain length between the nitrogens causes a much larger dissociation rate than in the EDTA system. In general, the rate of dissociation of various actinide amino polycarboxylates depends on the stereochemistry of the ligand and the relative basicities of the nitrogen atoms.

Acknowledgment. This research was supported by a contract at FSU with the USDOE, OBES, Division of Chemical Sciences.

Contribution from the Faculty of Pharmaceutical Sciences, Nagoya City University, Mizuho-ku, Nagoya 467, Japan

Conformational Interconversion Rates of 1,2-Diamine Chelates: Determination by Paramagnetic NMR Spectra of Low-Spin Iron(III) Complexes

Yoshitaka Kuroda, Noriko Tanaka, Masafumi Goto,* and Tomoya Sakai

Received July 15, 1988

The activation parameters for the $\delta \rightleftharpoons \lambda$ interconversion of the five-membered diamine chelate rings in $[Fe(CN)_4(1,2\text{-diamine})]^-$ have been determined from a line-shape analysis of the paramagnetic 1H NMR spectra by taking advantage of the large differences in chemical shift: $\Delta H^\ddagger = 24.7 \pm 4.5, 30.1 \pm 3.9, 42.7 \pm 2.0$ kJ mol $^{-1}$; $\Delta S^\ddagger = 0.0 \pm 27.0, -2.9 \pm 19.1, -7.7 \pm 8.4$ J K $^{-1}$ mol $^{-1}$; $\Delta G^\ddagger_{298} = 24.7 \pm 3.6, 31.0 \pm 1.8, 45.0 \pm 0.5$ kJ mol $^{-1}$ for ethanediamine, (2*R*,3*S*)-butanediamine, and (1*R*,2*S*)-*cis*-cyclohexanediamine. The effects of the alkyl groups on the rate of the interconversion are discussed. Temperature dependences of the paramagnetic shifts and the half line widths of the chelate ring protons for (*R*)-1,2-propanediamine and *N,N'*-dimethylethanediamine were measured, treated empirically, and employed for the calculation of the rate.

Introduction

Five-membered chelate rings formed by coordination of bidentate ligands, e.g., 1,2-diamines, diarsenes, thioethers, etc. to transition-metal ions have puckered conformations with either the δ or λ gauche form.¹ At room temperature the conformations of the chelate rings interconvert between δ and λ .^{2,3} The populations of the two conformers have been investigated for diamine complexes of Co^{III} ,⁴⁻¹¹ $Cr^{0,9,10}$ $Mo^{0,9}$ Ru^{II} ,^{5,12} Rh^{III} ,¹³ Pd^{II} ,^{4,9,14}

Pt^{II} ,^{4,9,15-22} Pt^{IV} ,^{5,18} Ni^{II} ,²³⁻³⁰ etc. by NMR spectroscopy. However, few informations about the dynamics of the conformational in-

- (1) Corey, J.; Bailar, J. C., Jr. *J. Am. Chem. Soc.* **1959**, *81*, 2620.
 (2) Hawkins, C. J.; Palmer, J. A. *Coord. Chem. Rev.* **1982**, *44*, 1.
 (3) Tapscott, R. E.; Mather, J. D.; Them, T. F. *Coord. Chem. Rev.* **1979**, *29*, 87.
 (4) Yano, S.; Ito, H.; Koike, Y.; Fujita, J.; Saito, K. *Bull. Chem. Soc. Jpn.* **1969**, *42*, 3184.
 (5) Beattie, J. K.; Novak, L. H. *J. Am. Chem. Soc.* **1971**, *93*, 620.
 (6) Sudmeier, J. L.; Blackmer, G. L.; Bradley, C. H.; Anet, F. A. *J. Am. Chem. Soc.* **1972**, *94*, 757.
 (7) Tiethof, J. A.; Cooke, D. W. *Inorg. Chem.* **1972**, *11*, 315.
 (8) Bagger, S.; Bang, O.; Woldbye, F. *Acta Chem. Scand.* **1973**, *27*, 2663.
 (9) Hawkins, C. J.; Peachey, R. M. *Aust. J. Chem.* **1976**, *29*, 33.

- (10) Toftlund, H.; Laier, T. *Acta Chem. Scand.* **1977**, *A31*, 651.
 (11) Hilleary, C. J.; Them, T. F.; Tapscott, R. E. *Inorg. Chem.* **1980**, *19*, 102.
 (12) Beattie, J. K.; Elsbernd, H. *J. Am. Chem. Soc.* **1970**, *92*, 1946.
 (13) Sudmeier, J. L.; Blackmer, G. L. *Inorg. Chem.* **1971**, *10*, 2010.
 (14) Pitner, T. P.; Martin, R. B. *J. Am. Chem. Soc.* **1971**, *93*, 4400.
 (15) Erickson, L. E.; McDonald, J. W.; Howie, J. K.; Clow, R. P. *J. Am. Chem. Soc.* **1968**, *90*, 6371.
 (16) Haake, P.; Turley, P. C. *J. Am. Chem. Soc.* **1968**, *90*, 2293.
 (17) Appleton, T. G.; Hall, J. R. *Inorg. Chem.* **1970**, *9*, 1807.
 (18) Appleton, T. G.; Hall, J. R. *Inorg. Chem.* **1971**, *10*, 1717.
 (19) Erickson, L. E.; Erickson, M. D.; Smith, B. L. *Inorg. Chem.* **1973**, *12*, 412.
 (20) Bagger, S. *Acta Chem. Scand.* **1974**, *A28*, 467.
 (21) Erickson, L. E.; Sarneski, J. E.; Reilley, C. N. *Inorg. Chem.* **1975**, *14*, 3007.
 (22) Lind, T.; Toftlund, H. *Acta Chem. Scand.* **1982**, *A36*, 489.
 (23) Ho, F. F.-L.; Reilley, C. N. *Anal. Chem.* **1969**, *41*, 1835.
 (24) Ho, F. F.-L.; Reilley, C. N. *Anal. Chem.* **1970**, *42*, 600.
 (25) Ho, F. F.-L.; Erickson, L. E.; Watkins, S. R.; Reilley, C. N. *Inorg. Chem.* **1970**, *9*, 1139.